Gas gain uniformity tests performed on multiwire proportional chambers for the LHCb muon system

A. Alves[a], L.M. de Andrade Filho[b], A.F. Barbosa[a], J.S. Graulich[c,1], G. Guerrer[a], H.P. Lima Jr.[a], K. Mair[c], E. Polycarpo[d,*,2], A. Reis[a], F. Rodrigues[d], B. Schmidt[c,**], T. Schneider[c], C. Schoch Vianna[d]

[a]Centro Brasileiro de Pesquisas Físicas, Brazil
[b]COPPE - UFRJ, Brazil
[c]CERN, CH 1211, Genève 23, Switzerland
[d]Instituto de Física/UFRJ, CP 68528, 21941-972, Rio de Janeiro, RJ, Brazil

Abstract

We present the experimental setup and the results of the gas gain uniformity tests performed as part of the quality control of the multiwire proportional chambers produced at CERN for the LHCb muon system. The test provides a relative gas gain measurement over the whole chamber sensitive area. It is based on the analysis of the pulse height spectrum obtained when the chamber is exposed to a ^{241}Am radioactive source. Since the measurement is normalized to the peak of a precise pulse generator, the gain uniformity can also be evaluated among different gas gaps and different chambers.

In order to cope with the specific requirements related to the relatively high number of chambers and to their varying geometry, a standalone and compact data acquisition system has been developed which is programmable at the hardware level and may be applied to many other applications requiring precise time-to-digital and analog-to-digital conversion, in correlated or non-correlated mode.
© 2008 Elsevier B.V. All rights reserved.

1. Introduction

The purpose of the LHCb muon System [1–3] is to provide fast triggering at the lowest trigger level and offline muon identification. The muon trigger demands a hit in five muon stations within the LHC bunch crossing interval of 25 ns. For each muon station, a minimum detection efficiency of 99% in a 20 ns time window is required. This requirement is achieved with a design where four chamber gaps are grouped together, each double-gap featuring at least 90% efficiency in that time window. Gas Electron Multiplier (GEM) and multiwire proportional chambers (MWPCs) demonstrated a satisfying ageing behavior and accomplish these stringent demands on fast triggering in a high rate environment [4,5].

1.1. Layout of the LHCb muon system

The five muon stations (M1–M5) of the LHCb detector are of rectangular shape, covering an acceptance of ±300 mrad (horizontally) and ±250 mrad (vertically). Each muon station is divided in four regions, R1–R4, with increasing distance from the beam axis, defining increasing angles from the interaction point. The chamber dimension and the pad segmentation size vary with the regions. The

---

first station (M1) is placed in front of the LHCb calorimeters and is equipped with GEM-chambers in the innermost region around the beam pipe and with double-gap MWPCs in the outer regions. Both detector types were designed to minimize the amount of material in front of the calorimeters. The other four stations (M2–M5) are placed after the Hadron Calorimeter (HCAL) and are interleaved with thick iron walls. They are equipped with four-gap MWPCs.

In total, the system is composed of 12 GEM plus 1368 MWPCs of 19 different sizes, with either anode or cathode readout, or simultaneous cathode and anode readout. Various production sites in Italy (LNF, Frascati, and Firenze), in PNPI at St. Petersburg, Russia, and at CERN participated in the construction of the MWPCs. CERN produced the chambers that cover 7 of the innermost regions of the muon system: M1R2 (muon station 1, region 2), M2R1, M2R2, M3R1, M3R2, M4R1 and M5R1.

1.2. Design of the four-gap multiwire proportional chambers (MWPCs)

Fig. 1 is a schematic side view of a typical four-gap LHCb muon chamber. The anode wire plane is made with
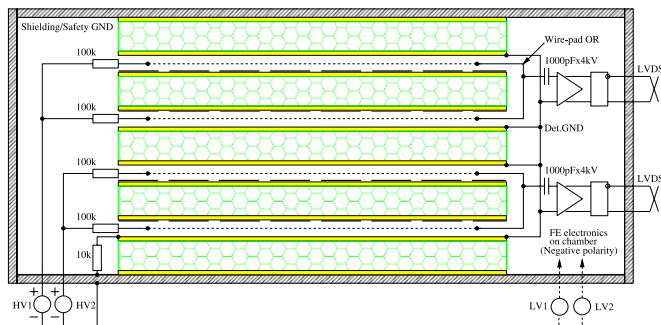

Fig. 1. Schematic view of a MWPC: sideview through the four gas gaps.

$30\,\mu m$ gold-plated tungsten wires, spaced by $2\,mm$ and centered in the $5\,mm$ gap between two cathode planes. For the chambers with wire readout, the wires are grouped together to form wire sensors of different sizes, defining 48 wire pads per gap (see Table 1). The cathode planes are segmented into cathode pads separated by a ground line. The pads are read out on both sides of the chamber. For M2R1 and M3R1, it has been shown that the signal-to-noise ratio improved when the signal is read out from two cathodes defining a gap in a hardwired OR (double cathode readout) [4]. For the chambers of the remaining types, only one cathode plane per gap is segmented into pads (single cathode readout).

According to their design M2 and M3 chambers can be grouped together as four-gap chambers with cathode and wire readout, M4 and M5 chambers are four-gap chambers with cathode readout. Table 1 summarizes the dimensions and segmentation sizes for each of the CERN-built chamber types.

The nominal gas mixture is $Ar/CO_2/CF_4$ (40/55/5). At the operational voltage of $2.65\,kV$ the gas gain is close to 5×10^4. Table 2 summarizes the design parameters of the MWPC.

1.3. Production and quality control

In order to guarantee a constant quality of the produced chambers and to allow fast tracing of potential production problems, precise procedures have been defined for each production step. In addition, six main quality control tests are performed at different stages of the production: wire fixation bar thickness, wire pitch, wire tension, gas leak rate, dark current and gas gain uniformity. The first five of them have been presented in [7]. In addition to the quality tests, the chambers undergo a conditioning procedure for anode and cathode cleaning [8].

Table 1
Dimensions and segmentation sizes of the different types of the CERN-built MWPCs

	Total # of chambers	Sensitive area (mm^2)	# of wire pads per gap, pad width (mm)	# of cathode pads per gap, pad area (mm^2)	# of FEBs per chamber
M1R2	24	484×200	24 (not read out)	24×8 20×25	24
M2R1	12	308×253	48 6–8	8×8 37.5×31.3	14
M2R2	24	612×253	48 12–14	8×8 75×31.3	14
M3R1	12	332×273	48 6–8	8×8 40.5×33.7	14
M3R2	24	660×273	48 12–14	8×8 80×33.7	14
M4R1	12	356×293	12 (not read out)	12×8 29×36	12
M5R1	12	380×313	12 (not read out)	12×8 31×39	12

Numbers are taken from [6].

Table 2
Design parameters for the MWPC for the LHCb muon system

Gas gap size	5 mm
Wire spacing	2 mm
Wire	Gold-plated tungsten
Wire diameter	30 μm
Wire length	250–310 mm
Mechanical wire tension	60 g
Gas mixture	$Ar/CO_2/CF_4$ (40/55/5)
Nominal HV	2650 V
Gas gain at nominal HV	5×10^4
Gas gain uniformity	Within 30%
Efficiency per double gap	$\geqslant 90\%$ in a 20 ns window

This article presents an innovative method, combining two well established techniques, namely time spectrum of delay lines signals and pulse height analysis, to measure the gas gain uniformity of the LHCb muon MWPC. The electronic device specifically developed to perform the data acquisition (DAQ) of the tests and results obtained for all CERN-produced chambers (except M1R2 chambers, where the proposed measurement could not be applied) are also reported.

2. Gas gain uniformity test

The gas gain uniformity measurement is based on the analysis of the pulse height spectrum obtained when a chamber is illuminated by a ^{241}Am radioactive source. This spectrum exhibits a peak in a position proportional to the gas gain. The peak results mainly from the absorption, in the chamber gas, of 8 keV fluorescence X-rays emitted by the copper atoms from the cathode plane when excited by the 60 keV emission line of the source. The 60 keV line also contributes with Compton scattering. In addition, there are other ^{241}Am characteristic emission lines at lower energies, around 14 keV. These have lower probability to penetrate the active gas volume. The observed peak shape is degraded by the relatively poor energy resolution of the chamber, but still it may be used as a reference, since its central position may easily be identified by a Gaussian fit, and it clearly varies with the applied voltage, i.e., with the chamber gain. The source activity (24 MBq) is low enough to minimize radiation safety issues, and the small size of the chambers allows the fixation of the source at a small distance (≈ 1 m) from which it is possible to illuminate the whole chamber.

The pulse height information is obtained by connecting together all the anode wires from one gap and amplifying the corresponding signal in one readout channel. The amplitude of the anode signal is then digitized with a sampling analog-to-digital converter (ADC).

The cathode signal is used to localize the detected X-ray photons on the surface of a gap plane. Each cathode pad of one-half of a gap is connected to a cell of a delay line. The delay line is read out at both ends. By comparing the arrival times of the cathode signal pair at each end of the

delay line, the cathode pad position is identified. In this way, only two pre-amplifiers are needed to read out a half gap. The signals are discriminated against electronic noise, and the time differences are digitized with a time-to-digital converter (TDC).

The DAQ system is able to synchronize, for each event occurring in the chamber, the time information and the pulse amplitudes obtained from the cathodes and the wires, respectively. The amplitude spectrum may therefore be registered for each pad of any of the four chamber gas gaps.

Details and preliminary results concerning the development of the test station based on these principles have been previously reported [9].

Although the method and the analog part of the system have remained essentially the same, the digital part has evolved from an experimental setup based on VME standard data processing units to a compact stand-alone unit communicating to a personal computer (PC). In the following sections we concentrate on the new DAQ aspects and on the presentation of final results.

2.1. The analog data processing modules

In Fig. 2 a schematic view of the test station signal processing stages is shown. The anode bar is a printed circuit board which provides the short-circuit of the whole anode wire plane. The anode signal is split in two after amplification, so that it can be simultaneously discriminated and analyzed with an ADC. The digital signals from the output of the discriminators are input to a TDC device, as start (anode) or stop signals (cathode). In order to readout the four chamber gaps, we require eight delay lines and 16 pre-amplifiers for the cathode signals, and four pre-amplifiers for the anode signals, as well as 20 discriminator channels. The modules used up to this point comprise the analog part of the DAQ setup. The pre-amplifier circuit has been developed specifically for this application [10]. The whole system is assembled on a metallic surface which is also the ground plane. The DAQ system is completed by a digital data processing sector to which converge all the signals from the previous modules.

2.2. The digital data processing module

A dedicated hardware using dual-ADC and TDC integrated circuits has been developed and implemented to process the DAQ operations involved in the chamber tests. A field programmable gate array (FPGA) has been introduced to manage the data flow control and storage. The resulting data processing module (DPM) incorporates all the functions related to the chamber gain uniformity measurements: it identifies the position of the cathode pad being hit by an ionizing event, and measures the anode pulse amplitude related to this event. A simplified diagram of the DPM circuit is shown in Fig. 3. The data readout is done by any standard PC, using the Enhanced Parallel Port
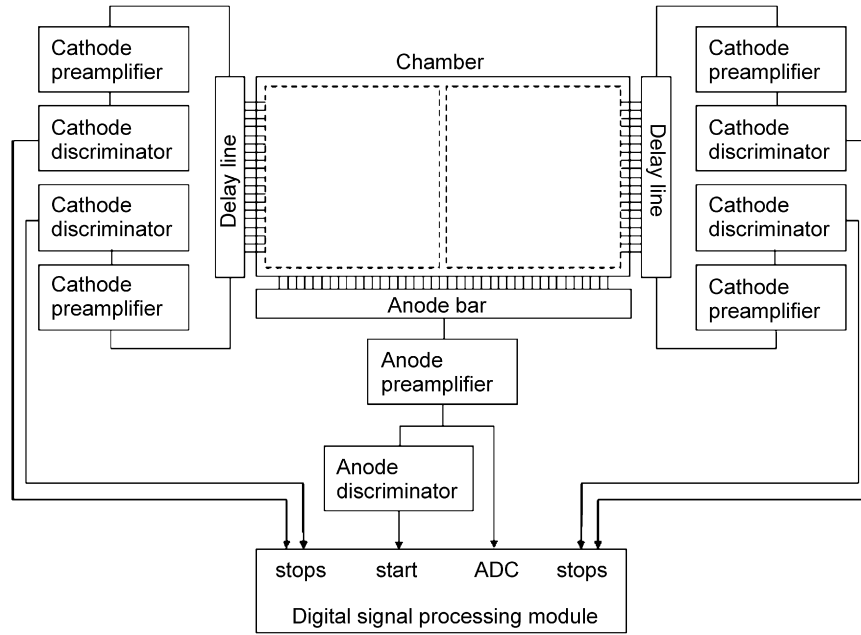
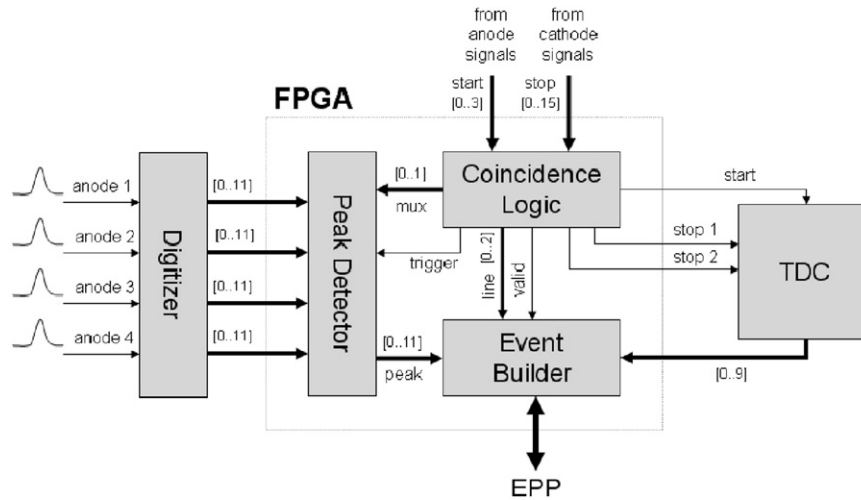Fig. 2. Schematic view of the analog modules in the test station setup.

Fig. 3. DPM functional block diagram.

(EPP) interface. The coincidence logic block in the DPM circuit triggers a peak detector state machine whenever any of the four start (anode) pulses is received from the readout electronics. It also triggers the event builder block if the corresponding event is considered as valid. An event is valid if it is associated to the detection of a photon originated from the radiation source, i.e., if it occurs in only one gap. This is so because we are only interested in those events related to low energy photon detection. A crossing muon, for example, leaves its track in more than one gap and is rejected. The coincidence logic block therefore allows the identification of the cathode (delay line) and the gap (anode) where an event occurs, so that only one start–stop TDC channel suffices to the timing readout of the whole chamber. These features are implemented with a FPGA internal look-up-table, which maps valid events among all possible input combinations.

The TDC block relies on one integrated circuit [11], which was initially developed to be used in the COMPASS experiment at CERN [12]. It includes eight conversion channels, with 120 ps resolution per channel. The resolution may be adjusted by software and calibrated by a quartz crystal using a phase-locked-loop (PLL) circuit. Under the configuration used in the DPM, the maximum data processing rate is 2 million events per second. The TDC is controlled by its configuration registers, and the configuration procedure is done by a serial bit stream using a specific protocol. In the current application this protocol was implemented by software sending the correct bitstream via the registers implemented in the FPGA.

In the digitizer block the anode analog signals are converted to digital and sent for further processing within the FPGA. It consists of four identical channels, each one equipped with a low distortion differential driver and a fast pipeline ADC. The latter is a dual free-running unit, featuring a high performance sample-and-hold amplifier and using a multi-staged pipelined architecture with output error correction logics. It provides 12-bit resolution at 65 mega samples per second. The clock signal to the ADCs is generated by the FPGA through the use of an external crystal oscillator and a PLL block. The analog-to-digital conversion may be disabled by a power-down input signal controlled by the FPGA. When enabled, each ADC channel continuously delivers a digitized stream of its corresponding anode signal to the peak detector block. This one seeks the highest sample value delivered by the ADC in a time window of 500 ns. This window is adequate to the shape of the typical anode pulse. A state machine mechanism, triggered by the coincidence logic block, is responsible for registering the anode signal maximum amplitude.

3. Data acquisition

The test of a chamber involves a number of steps: first the chamber is flushed with the operational gas mixture, then it is powered with the nominal high voltage (2650–2750 V) and connected to the analog DPMs driving the signals to the DAQ. From this point, the system is ready to be operated via the software package developed specifically to acquire data for the gas gain uniformity tests (see Section 4). The tasks performed during operation are briefly described in the next subsections.

3.1. Time filtering and mapping

The typical time spectrum obtained from the chamber delay lines is composed of a series of peaks (see Fig. 4), each one related to an individual cathode pad. The signal propagation time per delay line cell has been chosen to be approximately 5 times greater than the chamber time resolution, which is 4 ns (RMS) at 2.65 kV [5,9], so that the peaks are clearly separated from each other. The fact that all cathode signals have to travel through the delay line allows us to define a time filtering that reduces noise due to spurious events. If, instead of measuring cathode signal pair time differences, we measure the time sum, then a single peak should result, centered at the total delay line propagation time. Events lying outside the peak are necessarily spurious. The software includes a facility to scan the time sum spectrum and to define cuts to exclude events outside the sum peak.

With the time filtering active, the spectrum obtained for the time difference of the cathode signal pair shows very low background counts and sharp peaks which are easily associated to the cathode pads. The process of precisely defining the time window related to each cathode pad is
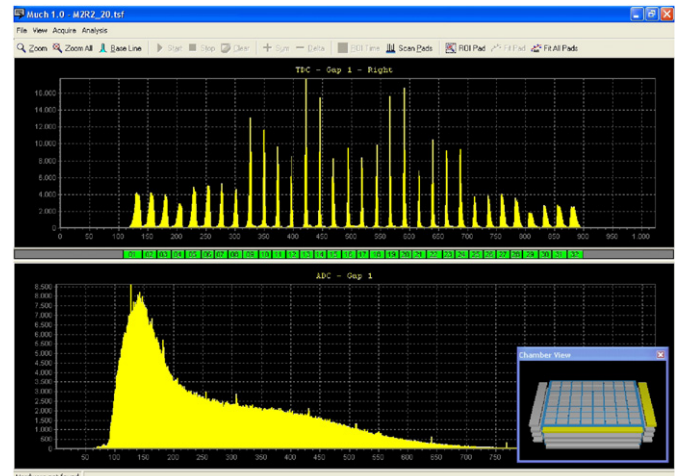

Fig. 4. A capture of the main window of the software showing the time-difference spectrum (top) and the anode pulse height spectrum (bottom). An interactive view of the chamber is also shown in the bottom right corner of the screen. It indicates that the data refer to the top gap and the right section of the chamber, which have both the anode bar and right delay line highlighted.

essentially a chamber mapping. The mapping information is required for assigning pulse height spectra to individual pads in the chamber.

3.2. Energy spectra acquisition

Once the above-mentioned time filtering and mapping are done for a chamber under test, data taking for the gain uniformity measurement may be started. The DAQ is switched to a mode where the time interval between cathode signal pairs is subtracted instead of summed. Then, for every valid detected event, the anode pulse amplitude and the cathode pair time difference are digitized. Data are stored in digital words containing the cathode pad number, the gap, and the pulse height of the event. An overall anode pulse height spectrum is registered in memory as a histogram, as well as individual pulse height spectra for every cathode pad in all gaps.

3.3. Data analysis

After the DAQ run, the same software (Section 4) prompts the user with the analysis tools. Basically, the user has to determine, from the overall anode pulse height spectrum, the area under which the ^{241}Am peak is centered. Then an algorithm searches for a peak under this area in all individual cathode pad pulse height spectra, and fits a Gaussian to each of them. The fit data may be seen and changed by the user, so that the fit quality can be interactively improved. The results are shown under different graphical visualizations, a data file is saved and a test report is generated. The analysis may be worked out off line whenever it is necessary, by accessing the chamber data file.

4. Software

An user-friendly software package [9] has been developed and made available to the chambers test station, implementing the control and the access to all the facilities referred to in the previous sections. It provides a step by step procedure to test a muon chamber. The main page of its graphical user interface is shown in Fig. 4.

In addition to the implementation of the hardware capabilities, the software also plays an essential role in the gain uniformity measurement. Three main software tools may be quoted as examples:

(1) *Gain normalization*: It is mandatory to take into account the pre-amplifier gain in the anode pulse amplitude measurement. One pre-amplifier is assigned to each of the four anode planes in the chamber, and their gains are not necessarily the same. The normalization procedure makes use of a periodic signal (a square wave, generated by a waveform generator) of fixed amplitude. This signal is input to each of the pre-amplifiers and a gain factor is obtained, which is

applied as a correction to the measured amplitudes. A specific part of the software acquires the response of the pre-amplifiers to the standard waveform, and saves it for the data analysis process. The pulse height spectra of a chamber may then be normalized to a standard, and this allows one to compare different gaps and even different chambers.

(2) *Base line correction*: Given an event counting rate, there is a probability that an event will be detected while the previous one has not yet been completely neutralized in the chamber. This causes piling up of signals and translates into an average base-line at the pre-amplifier output which is not at the ground level. This offset is the actual base-line amplitude, and has to be corrected for when an amplitude histogram is obtained. In order to evaluate the base-line offset, a specific software tool is used, under which a histogram is filled with anode signals not belonging to the triggered event. In other words, the trigger from a valid event occurring in one gap is used to readout the signal (i.e. the base-line) from the other three gaps. In this way, four base-line amplitude histograms are obtained, one for each gap. A Gaussian fit is applied to the peaks in each of the histograms, and the chamber gas gain is corrected for by this offset level.

(3) *Report generation*: The final output of the test is a report including a series of graphics related to the relevant parameters of the gain measurement. The generation of the results registered in the reports is done by software algorithms that compute the parameters related to the chamber gain distribution. Both, the raw and the analyzed data are shown, as well as important statistical information that precisely characterize the tested chambers.

Figs. 5–9 illustrate the kind of data available in the report file, for the case of a typical chamber. The different parameters of the fit can be seen as a two-dimensional plot representing the chamber surface (Fig. 5), as a function of the pad number for all pads in one gap (Fig. 6) or displayed in a histogram (Fig. 7). The χ^2 of the fit and the remaining parameters can also be visualized, as well as their errors (Figs. 8–9).
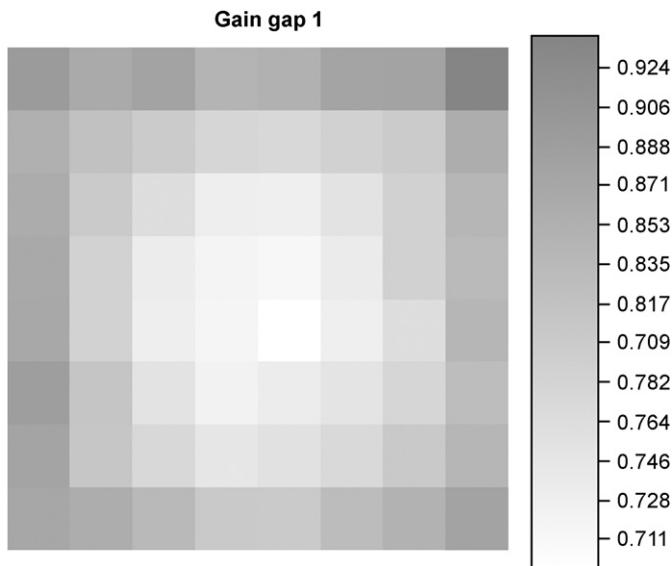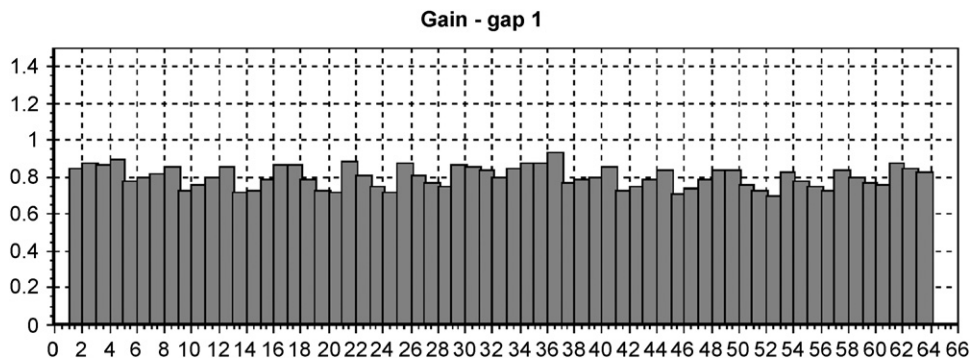

Fig. 5. Normalized gain over the cathode pads.

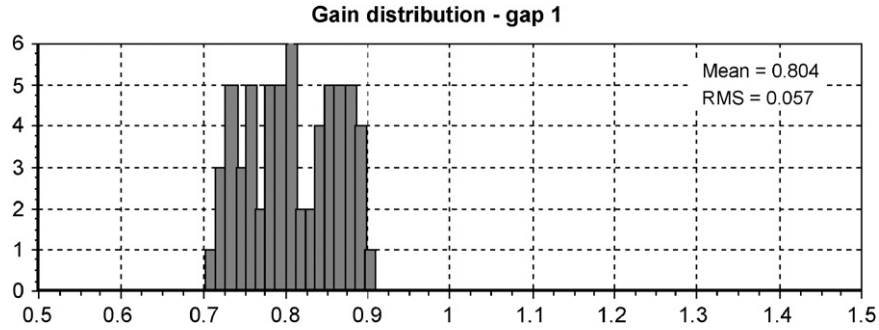Fig. 6. Normalized gain as a function of the pad number.

Gain distribution - gap 1

Mean = 0.804
RMS = 0.057

Fig. 7. Histogram of the normalized gain in one gap.

Chi2 – gap 1

Fig. 8. χ^2 of the Gaussian fit as a function of the pad number.

Mean Error – gap 1

Fig. 9. Error on the peak mean value as a function of the pad number.

5. Results

The results here presented refer to six classes of chambers produced at CERN for the LHCb muon system. The test is supposed to qualify the chambers concerning the gain uniformity. For this purpose, the gain over all pads of each chamber is measured. Gaps #1 and #2 are grouped together and labeled as 'bi-gap 1', while gaps #3 and #4 are labeled as 'bi-gap 2'. The average normalized gain is computed for all pads in bi-gaps 1 and 2. The specification for the gas gain uniformity per bi-gap requires a gain variation smaller than 30% for 95% of the surface [7]. In order to classify the performance of the chambers two intervals A and B around the average gas gain per gap have been defined: interval A: $\overline{G}/\sqrt{2} \leqslant G(x,y,) \leqslant \sqrt{2} \cdot \overline{G}$ and interval B: $\overline{G}/\sqrt{2} \leqslant G(x,y,) \leqslant \sqrt{2} \cdot \overline{G}$, where $\overline{G}$ is the average gas gain per bi-gap and $G(x,y,)$ is the gas gain on a certain position in x and y on the gap surface. The corresponding voltage range is ± 53 and ± 84 V for interval A and B, respectively [13]. A chamber is classified as *good* if the combination of both bi-gaps shows a gas gain uniformity within interval AA (for bi-gaps 1 and 2), AB or BA, and as *reserve* if the uniformity is within BB. A chamber with a gas gain variation larger than interval B is rejected and classified as *failure*.

In Fig. 10, the results for one class of chambers are shown. The dotted and the solid lines indicate the limits of interval A and B, respectively. In this particular case (M2R2 chambers), some units were tested with both the DPM and the VME-based setups (see Section 2). The results are in good agreement, indicating the reliability of the method and of its implementation.
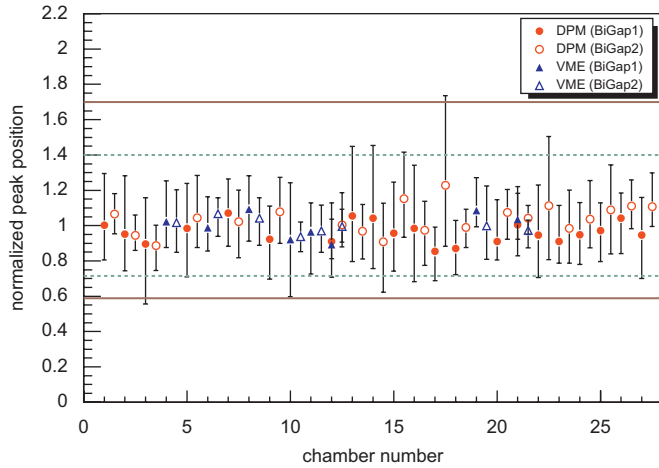
Fig. 10. Results for the M2R2 chambers normalized gas gain as a function of chamber number. Filled and empty symbols correspond to bi-gaps 1 and 2, respectively. Triangles are used for chambers tested with the new DAQ (DPM) and circles are used for the previous system based on the VME standard. The error bars represent the minimum and maximum values of the normalized gas gain in the corresponding bi-gap. Chambers 12 and 21 are tested with both DAQ versions.

Table 3
Number of chambers classified in the different categories

Type	Classification with fixed HV			Classification with adjusted HV		
	Good	Reserve	Failure	Good	Reserve	Failure
M2R1	15	0	1	16	0	0
M2R2	24	1	2	27	0	0
M3R1	14	0	0	14	0	0
M3R2	26	0	0	26	0	0
M4R1	13	2	1	16	0	0
M5R1	12	3	2	17	0	0

After fine adjustment of the high voltage in each individual gap, all chambers are classified as 'good'.

The test was applied to all the chambers, and these were rated as good, reserve or failing, according to the above-mentioned criterium. In Table 3 the results are summarized. It has to be noted that same high voltage was applied to both bi-gaps in each chamber. However, when adjusting the high voltage for each gap within the range of ±50 V, the small number of failing chambers (6 out of 116) are accepted as 'good' chambers.

This is visualized in Fig. 11. Fig. 11(a) shows the result of the gas gain for M5R1 chambers per bi-gap. Two bi-gaps exceed the acceptance limit. When plotting the gas gain for each of the four gaps individually (Fig. 11(b)), it can be seen that the uniformity within one gap is well within the acceptance, if the mean value is adjusted. By regulating the high voltage for each gap, all chambers will show a gas gain uniformity within the acceptance range, and can therefore be classified as 'good' (see Table 3).

The quantitative details related to all the tested chambers are presented in Table 4. No correction for temperature or atmospheric pressure has been applied to the measurements, since the variations from test to test were comparable to the
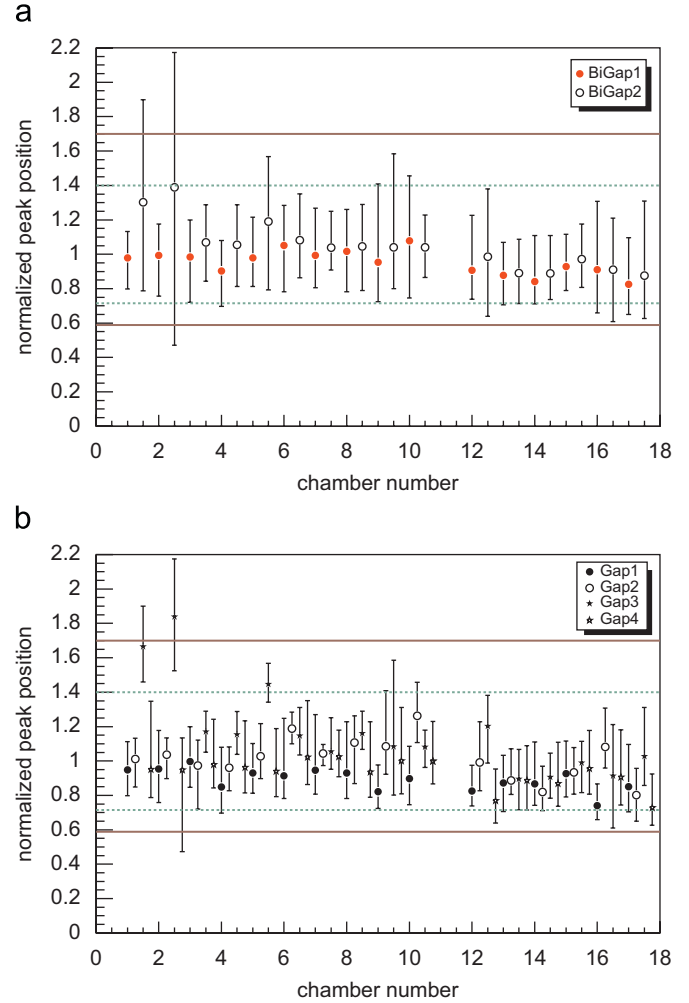

Fig. 11. Gas gain uniformity results for M5R1 chambers: (a) shows the gas gain per bi-gap, with two bi-gaps exceeding the specified acceptance limit. (b) shows the gas gain per gap without adjusting the high voltage for each gap. Chamber 11 has been rejected due to a gas leak.

Table 4
Mean and RMS values of the normalized gas gain distributions for the different chamber types

	Bi-gap 1		Bi-gap 2	
	Mean	RMS	Mean	RMS
M2R1	0.949	0.068	1.051	0.073
M2R2	0.978	0.066	1.022	0.069
M3R1	1.005	0.085	0.996	0.051
M3R2	1.032	0.067	0.968	0.053
M4R1	0.987	0.051	1.013	0.101
M5R1	0.951	0.069	1.049	0.140

variations within the test duration (temperature RMS smaller than 3 °C and pressure RMS smaller than 5 mbar).

6. Conclusions

A gas gain uniformity test setup for the LHCb muon chambers produced at CERN has been developed and the

chambers have been tested with two DAQs: a VME based system and the dedicated data processing module (DPM).

CERN has produced 116 chambers for muon stations M2–M5, which passed all preceding quality tests and were tested for gas gain uniformity. Out of them, one third were tested with the VME based system, while two thirds were tested with the DPM. The two chambers tested with both DAQ systems showed good agreement, confirming the reliability of the method. As shown in Table 1, only 96 MWPCs are needed to instrument the corresponding regions of the LHCb muon system. Since all 116 tested chambers present a gas gain uniformity which classifies them as 'good', the 20 remaining chambers are taken as spare detectors, to be used in case of failures during operation. Between two and five good quality spare chambers are available per region.

References

[1] LHCb Collaboration, LHCb Muon System TDR, CERN-LHCC-2001-010, May 2001.

[2] LHCb Collaboration, LHCb Muon System TDR Addendum 1, CERN-LHCC-2003-002, January 2003.

[3] LHCb Collaboration, LHCb Muon System TDR Addendum 2, CERN-LHCC-2005-012, April 2005.

[4] A. Kachtchouk, et al., Nucl. Instr. and Meth. A 555 (2005) 48.

[5] G. Lanfranchi, Nucl. Instr. and Meth. A 535 (2004) 221.

[6] W. Riegler, Crosstalk, cathode structure and electrical parameters of the MWPCs for the LHCb muon system, LHCb Muon 2000-061, April 2003.

[7] A.F. Barbosa, et al., IEEE Trans. Nucl. Sci. NS-53 (2006) 336.

[8] J.-S. Graulich, et al., Conditioning of MWPCs for the LHCb muon system, in: 2005 IEEE Nuclear Science Symposium Conference Record, vol. 3, 2005.

[9] A. Alves et al., Results of the MWPC gas gain uniformity tests performed at CERN, LHCb 2007-115, August 2007.

[10] A.F. Barbosa, R. da Silva, Nucl. Instr. and Meth. A 555 (2005) 93.

[11] ⟨http://www.acam.de⟩ (F1 datasheet, scientific version).

[12] G. Braun, et al., F1—an eight channel time-to-digital converter chip for high rate experiments, in: Proceedings of the 5th Workshop Electronics for the LHC Experiments—LEB99, CERN/LHCC/99-33, 1999.

[13] S. de Capua, Study of gas gain uniformity of the LHCb muon system MWPCs using cosmic rays, LHCb-Muon 2006-010, March 2006.